J. Membrane Biol. 193, 35–45 (2003)
DOI: 10.1007/s00232-002-2005-5

The Journal of
Membrane
Biology

Copper Modulation of Ion Channels of PrP[106–126] Mutant Prion Peptide Fragments

J.I. Kourie[1], B.L. Kenna[1], D. Tew[2], M.F. Jobling[2], C.C. Curtain[2], C.L. Masters[2], K.J. Barnham[2], R. Cappai[2]
[1]Membrane Transport Group, Department of Chemistry, The Faculties, The Australian National University, Canberra City, Australian Capital Territory, 0200 Australia
[2]Department of Pathology, The University of Melbourne, 3010 and The Mental Health Research Institute, Parkville, 3052 Victoria, Australia

Received: 1 November 2002/Revised: 22 January 2003

Abstract. We have shown previously that the protease-resistant and neurotoxic prion peptide fragment PrP[106–126] of human PrP incorporates into lipid bilayer membranes to form heterogeneous ion channels, one of which is a Cu^{2+}-sensitive fast cation channel. To investigate the role of PrP[106–126]'s hydrophobic core, AGAAAAGA, on its ability to form ion channels and their regulation with Cu^{2+}, we used the lipid-bilayer technique to examine membrane currents induced as a result of PrP[106–126] (AA/SS) and PrP[106–126] (VVAA/SSSS) interaction with lipid membranes and channel formation. Channel analysis of the mutant (VVAAA/SSS), which has a reduced hydrophobicity due to substitution of hydrophobic residues with the hydrophilic serine residue, showed a significant change in channel activity, which reflects a decrease in the β-sheet structure, as shown by CD spectroscopy. One of the channels formed by the PrP[106–126] mutant has fast kinetics with three modes: burst, open and spike. The biophysical properties of this channel are similar to those of channels formed with other aggregation-prone amyloids, indicating their ability to form the common β sheet-based channel structure. The current-voltage (*I-V*) relationship of the fast cation channel, which had a reversal potential, E_{rev}, between −40 and −10 mV, close to the equilibrium potential for K^+ (E_K = −35 mV), exhibited a sigmoidal shape. The value of the maximal slope conductance (g_{max}) was 58 pS at positive potentials between 0 and 140 mV. Cu^{2+} shifted the kinetics of the channel from being in the open and "burst" states to the spike mode. Cu^{2+} reduced the probability of the channel being open (P_o) and the mean open time (T_o) and increased the channel's opening frequency (F_o) and the mean closed time (T_c) at a membrane potential (V_m) between +20 and +140 mV. The fact that Cu^{2+} induced changes in the kinetics of this channel with no changes in its conductance, indicates that Cu^{2+} binds at the mouth of the channel via a fast channel block mechanism. The Cu^{2+}-induced changes in the kinetic parameters of this channel suggest that the hydrophobic core is not a ligand Cu^{2+} site, and they are in agreement with the suggestion that the Cu^{2+}-binding site is located at M_{109} and H_{111} of this prion fragment. Although the data indicate that the hydrophobic core sequence plays a role in PrP[106–126] channel formation, it is not a binding site for Cu^{2+}. We suggest that the role of the hydrophobic region in modulating PrP toxicity is to influence PrP assembly into neurotoxic channel conformations. Such conformations may underlie toxicity observed in prion diseases. We further suggest that the conversions of the normal cellular isoform of prion protein (PrP^c) to abnormal scrapie isoform (PrP^{Sc}) and intermediates represent conversions to protease-resistant neurotoxic channel conformations.

Key words: Neurodegenerative diseases — Transitional metals — Ion channel pathologies — Calcium homeostasis — Membrane damage — Protein misfolding — Amyloids

Introduction

Prions are the infectious agent responsible for transmissible spongiform encephalopathies (TSEs) such as Creutzfeldt-Jakob disease and bovine spongiform encephalopathy (Prusiner et al., 1998). This infectious

Correspondence to: J.I. Kourie; email: Joseph.Kourie@anu. edu.au

Abbreviations: Aβ, amyloid β-peptide; CD, circular dichroism spectroscopy; PrP, prion protein; PrP^c, normal cellular form of prion proteins; TSE, transmissible spongiform encephalopathy

Table 1. Peptide names, sequences, and abbreviations used in this study

Peptide	Peptide sequence	Abbreviation
PrP106–126	KTNMKHMAGAAAAGAVVGGLG	
PrP106–126 A118S/A117S	KTNMKHMAGAA**SS**GAVVGGLG	AA/SS
PrP106–126V122S/V121S/A118S/A117S	KTNMKHMAGAA**SS**GA**SS**GGLG	VVAA/SSSS
PrP106–126 scrambled sequence	NGAKALMGGHGATKVMVGAAA	Scrambled

Mutations were undertaken to alter the hydrophobicity of the central core of the WT PrP[106–126] peptide. The mutated serines are in bold.

agent appears to be composed exclusively of the prion protein (PrP), a molecule that has acquired a toxic infectious conformation. Several hypotheses have been proposed to explain prion-induced neurodegenerative diseases (for review, *see* Kourie, 2001). These include changes in: (i) membrane microviscosity; (ii) intracellular Ca^{2+} homeostasis; (iii) the function of PrP as a superoxide dismutase and a modulator of Cu^{2+} homeostasis; and (iv) the immune system. The prion-induced modification in Ca^{2+} homeostasis has been proposed to be the result of: (1) prion interaction with intrinsic ion transport proteins, e.g., L-type Ca^{2+} channels in the surface membrane; K^+/Na^+-ATPase; Na^+-glutamate; NMDA receptors and IP_3-modulated Ca^{2+} channels in the internal membranes (*see* Kourie, 2001 and references therein), and/or (2) formation of β barrel-based ion channels (Lin, Mirzabekov & Kagan, 1997, Hirakura et al., 2000, Kourie & Culverson, 2000). These two mechanisms of prion action lead, directly or indirectly, to changes in Ca^{2+} homeostasis that further augment the abnormal electrical activity and distortion of the signal transduction pathways leading to cell death.

The prion protein (PrP) can exist in either a normal cellular form (PrP^c) or an abnormal disease-associated form (PrP^{TSE}) . Spectroscopic studies have shown that PrP^c contains 40% α-helix and minimal β-sheet content, whereas PrP^{TSE} contains 43% β-sheet and a reduction of α-helix to 30% (Pan et al., 1993). Elucidating the conformational changes that occur during the production of PrP^{TSE} is central to understanding the mechanisms of prion diseases. The peptide fragment encompassing residues 106–126 of human PrP is highly fibrillogenic and toxic to neurons in vitro (Forloni et al., 1993; Brown, Herms & Kretzschmar, 1994; Stewart et al., 2001; Tagliavini et al., 2001) and has the ability to form ion channels (Lin et al., 1997; Kawahara et al., 2000; Kourie & Culverson, 2000). The PrP[106–126] peptides contain the highly hydrophobic segment AGAAAAGA from positions 113 to 120 (Tagliavini et al., 2001), which can confer on the fragment the ability to interact with lipid membranes and form ion channels (Kourie 2001; Kourie et al., 2001a). The toxic effects of PrP[106–126] on neuronal cells and its ability to induce apoptosis (Forloni et al., 1993; Brown et al., 1994; Brown, Clive & Haswell, 2001; White et al., 2001), as well as its ability to mimic the toxicity of PrP^{TSE} to cause cell death (Brown et al., 1994; Jobling et al., 1999; Gu et al., 2002; Singh et al., 2002), makes it a suitable investigative tool in prion research.

The PrP[106–126] ion channels in lipid bilayers are heterogeneous. This probably reflects modifications in the peptide's structure and differences in the properties of the formed oligomeric aggregates and their intermediates. Modulation of these channels by changes in the homeostasis of the brain's transition metals (e.g., Cu^{2+}), which have been linked to neurodegenerative diseases, is not known (Bush, 2001). In the case of prion diseases, it is thought that normal PrP functions as a metallochaperone in Cu^{2+} transport and homeostasis, and that this is altered in the disease state (*see* review by Wong et al., 2000). In turn, changes in Cu^{2+} homeostasis would affect the function of PrP. The effects of Cu^{2+} on PrP might be due to its ability to modify the secondary structure and enhance aggregation of the protein and hence its relative proteinase-K sensitivity (*see* Wong et al., 2000). The aims of this study were to: (*a*) test the ability to form channels with mutant PrP [106–126] isoforms that have a reduced hydrophobicity, using the PrP[106–126] (AA/SS) and PrP[106–126] (AAVV/SSSS) peptides; and (*b*) examine whether the mutants affect the modulation of these ion channels by Cu^{2+}.

Materials and Methods

Peptide Synthesis

The manual synthesis of PrP[106–126] has been reported previously (Jobling et al., 1999, 2001). The PrP[106–126] (AA/SS) mutant was synthesized by manual Boc chemistry with in situ neutralization, with a synthesis yield of 30%. PrP[106–126] (VVAA/SSSS) and PrP[106–126] (Scrambled) were synthesized by automated Fmoc chemistry with yields of 61 and 65%, respectively. The wild-type PrP[106–126] and its mutant peptides (Table 1) were purified by reverse-phase HPLC and their authenticity confirmed by MALDI-TOF mass spectrometry.

Lipid Bilayer Technique

Bilayers were formed across a 150 μm hole in the wall of a 1 ml delrin™ cup using a mixture of palmitoyl-oleoyl-phosphatidylethanolamine, palmitoyl-oleoyl-phosphatidylserine and palmitoyl-oleoyl-phosphatidylcholine (Miller & Racker, 1976; Kourie et al., 1996), obtained in chloroform from Avanti Polar Lipids (Alabas-

ter, AL). It has been suggested that the membranes can play a role in PrP^{Sc} dimerization through biasing the orientation and configuration of the PrP^{Sc} and that dimerization is enhanced by the lysine residues 101, 104 and 106 (Warwicker, 1999). To exclude the role of the variations arising from different membrane compositions in the formation of distinct PrP[106–126] channels, ionic currents were recorded from bilayers made of a single lipid mixture, i.e., PE:PS:PC, 5:3:2 (by volume). The lipid mixture was dried under a stream of N_2 gas and redissolved in *n*-decane at a final concentration of 50 mg/ml. Synthetic PrP[106–126], which has three amino acids with a net charge of +2 at pH >7 (obtained from Bachem, Switzerland), was dissolved in 250 mM KCl, divided into aliquots and kept at −84°C until use. The side of the bilayer to which the peptide or liposomes were added was defined as *cis*, and the other side as *trans*. The peptide was incorporated into the negatively charged lipid bilayer by addition of microliter aliquots of the dissolved peptide to the *cis* chamber at a final peptide concentration of 0.1–1 μg/ml. Ion channels were also recorded from a peptide:lipid mixture of 1:50. Unless stated otherwise, the initial experimental solution for incorporating synthetic PrP[106–126] into the bilayers contained KCl (250 mM *cis* and 50 mM *trans*), 1 mM $CaCl_2$, 10 mM HEPES and was adjusted to pH 7.4 with KOH. The experiments were conducted at 20 to 25°C.

Preparation of Liposomes

In some experiments liposomes of PrP[106–126] and its mutants were used. The method for the preparation of these liposomes was described by Arispe, Pollard and Rojas (1996). A 20 μl aliquot of palmitoyl-oleoyl-phosphatidylserine dissolved in chloroform (10 mg/ml) was placed in a glass tube. After evaporation of the chloroform (by blowing filtered N_2 gas into the tube), a 30 μl aliquot of 1 M potassium aspartate (pH adjusted to 7.2) was added and the resulting mixture was sonicated for 5 min. Next, a 20 μl (2 mg/ml) stock solution of the PrP[106–126] or of its mutants in water was added and the adduct was sonicated for two further minutes.

Ion Channel Recording

The pClamp-6 program (Axon Instruments) was used for voltage command and acquisition of ionic current families with an Axopatch 200 amplifier (Axon Instruments). The current was monitored with an oscilloscope and the data stored on computer. The *cis* and *trans* chambers were connected to the amplifier head stage by Ag/AgCl electrodes in agar salt bridges containing the solutions present in each chamber. Membrane voltages (V_m) and currents were expressed relative to the *trans* chamber. An outward current is defined as a cation moving from the *cis* to the *trans* chamber or an anion moving from the *trans* to the *cis* chamber. Data were filtered at 1 kHz (4-pole Bessel, −3 dB) and digitized via a TL-1 DMA interface (Axon Instruments) at 2 kHz.

Data Analysis

Modifications in the bilayer thickness, mediated via lipid solvents, e.g., *n*-decane, contribute to changes in channel gating kinetics of ion channels (Kourie, 1996) and particularly those formed with short peptides, e.g., the 15-amino-acid gramicidin-formed channel (Mobashery, Nielsen & Andersen, 1997). Therefore, standardizing the specific membrane capacitance (C_b) and its time independence is important in comparative and detailed investigations of ion channel characteristics. Kinetic analysis of the channels formed by the 21-amino-acid PrP[106–126] was conducted only for optimal bilayers having a C_b of >0.42 μF/cm^2 and which contained a single active channel. The criteria for defining ion currents as belonging to a "single channel" have been described elsewhere (Patlak, 1993). Single-channel activity was analyzed for overall characteristics using the program CHANNEL 2 (developed by P.W. Gage and M. Smith, *see* (Kourie et al., 1996)). CHANNEL 2 allows online analysis of the entire current record for computation of the mean current (I'). I' is defined as the integral of the current passing through the channel divided by the total time. The integral current is determined by computation of the area between a line set on the noise of the closed state and channel opening to various levels. The threshold level for the detection of single-channel events was set at 50% of the maximum current (Colquhoun & Hawkes, 1983). The maximal current (I) is the current amplitude of a fully open channel. The maximal current was obtained by measuring the distance (in pA) between two lines, one set on the noise of the closed level where the current amplitude is 0 pA and the other set on the noise of the majority of distinct events that were in the open state. The maximal current was also obtained by measuring the distance (in pA) between the peak at 0 pA (representing the closed state) and the extreme peak on the right (representing the open state) in the all-point histogram generated using CHANNEL 2 (*see* Kourie et al., 1996). Both methods were used and the results were generally in agreement. The E_{rev} was corrected for liquid junction potentials, using appropriate ionic mobilities (Barry, 1994). Each channel was used as its own control and the comparison was between conductance and kinetic parameters of the same channel recorded at different V_m before and after the channel was subjected to any treatment. Data reported are the means ± SEM, and the difference in means was analyzed by Student's *t*-test. Data were considered statistically significant when P values were ≤ 0.05.

Preparation of LUVs

The CD data for PrP[106–126] and its mutants were obtained in the presence of large unilaminar vesicles (LUVs). Synthetic palmitoyl phosphatidyl choline (POPC) was purchased from Sigma, and palmitoyl phosphatidyl serine (POPS) was purchased from Avanti Polar Lipids. The LUVs were prepared by dissolving equal quantities of POPS and POPC in chloroform, which was then evaporated off. The lipids were then dissolved in 10 mM phosphate buffer at pH 6.8. Some glass beads were added and the mixture was shaken for 1 h at 37°C. The solution was decanted from the glass beads and extruded 11 times through a 0.2 μm pore filter from Millipore, using an Avanti "mini-extruder" apparatus. The large unilaminar vesicles were stored at 4°C and used within 48 h of preparation.

CD Spectroscopy

The PrP[106–126] and its mutant were dissolved in LUVs (2 mg/ml, giving a molar ratio of 30:1 LUV:peptide) in the absence or presence of Cu^{2+} (molar ratio 1:1 Cu^{2+}:peptide). The CD spectra were obtained using a Jasco 810 spectropolarimeter at 37°C. Far-UV CD spectra were from 190 to 260 nm with a 0.1 cm path length. The concentration of protein used was 0.32 mg/ml, determined using the molar extinction coefficient of the UV absorption. The baseline acquired in the absence of peptide was subtracted and the resulting spectra were smoothed.

Results

Synthesis of PrP[106–126] and Hydrophobic Core Mutants

To determine the contribution of the hydrophobic core sequence AGAAAAGAVV of PrP[106–126] to

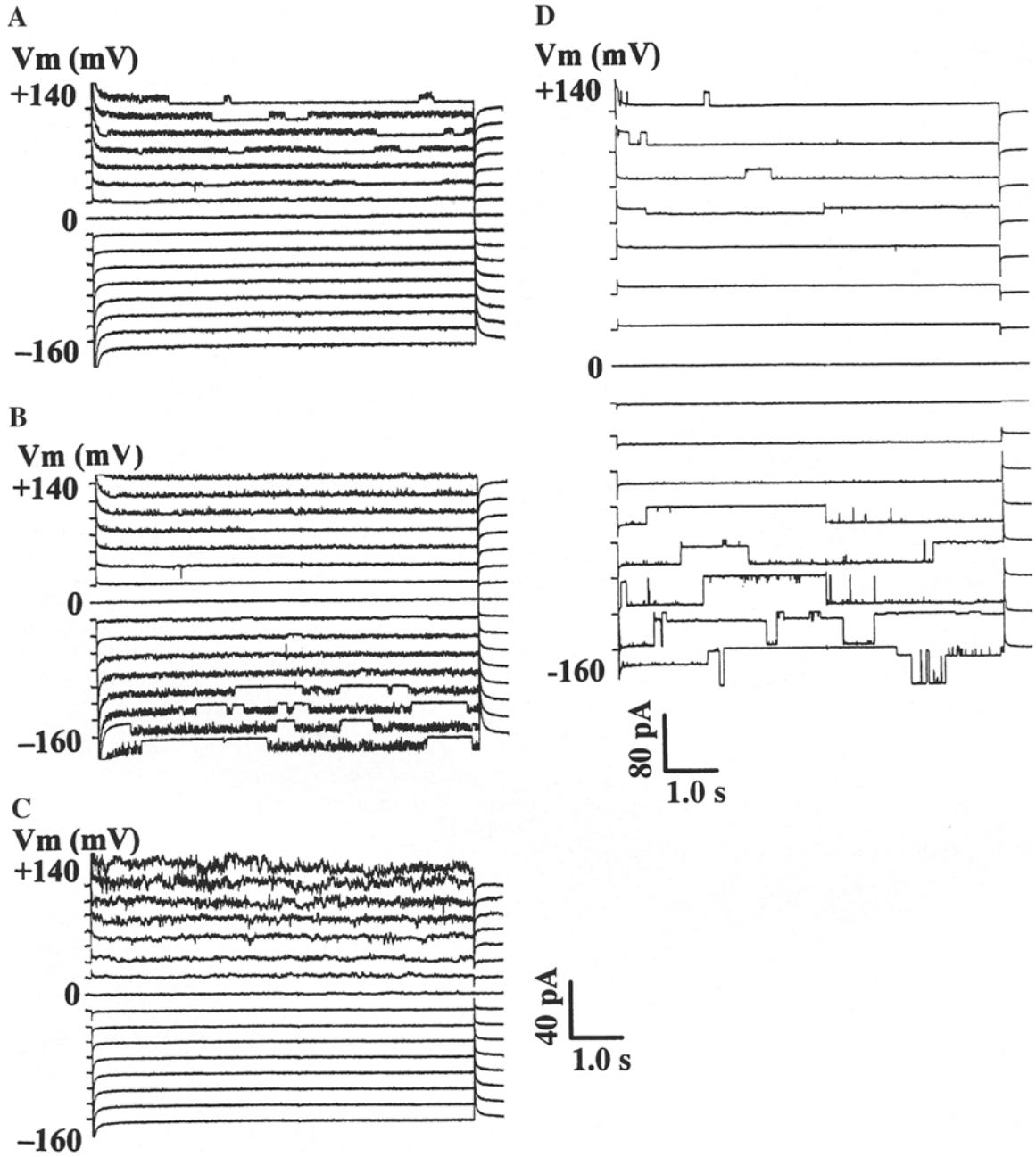

Fig. 1. Channel types formed by PrP[106–126] (AA/SS). Representative current traces, recorded for channels in different bilayers, illustrating the activity of ionic currents of: (*A*) PrP[106–126] WT outwardly-directed current with fast kinetics (*see* also Figs. 2*A*, *B* and 3*A* for indistinguishable PrP[106–126] (AA/SS) outwardly-directed currents with fast kinetics), (*B*) PrP[106–126] (AA/SS) inwardly-directed current with fast kinetics, (*C*) PrP[106–126] (AA/SS) irregular spike current, (*D*) PrP[106–126] (AA/SS) inactivating currents. All channels were recorded from voltage-clamped optimal bilayers, i.e., specific bilayer capacitance $> 0.42\ \mu F/cm^2$, at voltages between −160 and +140 mV. The *cis* solutions were 250 mM KCl and the *trans* solution was 50 mM KCl. Following convention, the upward deflections denote activation of outward potassium current, i.e., potassium ions moving from the *cis* chamber to the *trans* chamber. For a better display, the data are filtered at 1 kHz, digitized at 2 kHz and reduced by a factor of five.

the activity of channels formed by PrP[106–126] and to the channels' regulation, PrP[106–126] mutants were synthesized as detailed previously (Jobling et al., 1999). Briefly, by substituting the hydrophilic amino-acid residue serine for the hydrophobic residues alanine and valine, the hydrophobicity of the PrP[106–126] peptide was reduced. Serine is usually used as the substituting amino acid, as it introduces a non-charged amino acid of reasonably small size and minimized possible steric hindrance of peptide folding. These mutant peptides display reduced aggregation and are non-toxic in cell culture (Jobling et al., 1999).

Table 2. Distribution of the observed PrP[106–126] (AA/SS), PrP[106–126] (VVAA/SSSS) and PrP[106–126] (Scrambled) currents

Peptide	Outwardly-directed current[a] 103 channels	Inwardly-directed current[a] 18 channels	Outwardly-directed irregular "spiky" currents[a] 166 channels	Time-dependent inactivating channel[a] 34 channels	Distribution of the total (100%) of 321 channels
PrP[106–126] WT	57 (55%)	9 (50%)	47 (28%)	24 (71%)	137 (42.6%)
PrP[106–126] (AA/SS)	34 (33%)	1 (6%)	59 (36%)	2 (6%)	96 (29.9%)
PrP[106–126] (AAVV/SSSS)	12 (12%)	8 (44%)	60 (36%)	8 (23%)	88 (27.4%)
PrP[106–126] (Scrambled)	0 (0%)	0 (0%)	0 (0%)	0 (0%)	0 (0%)

[a] *See* Fig. 1 and text for definition. The channels were obtained from 10 lots of 20 attempts to incorporate each mutant peptide into optimal bilayers in the presence of 250/50 mM KCl in *cis/trans* chambers, respectively. For the PrP[106–126] (Scrambled), a total of 30 attempts was made. The same voltage protocol was used in each case to clamp the bilayer between voltages of −160 and +140 mV, in steps of 20 mV.

Channels Formed by PrP[106–126] (AA/SS) and PrP[106–126] (VVAA/SSSS)

One hundred and eightyfour channels were recorded after mutant incorporation into bilayers: PrP[106–126] (AA/SS), 96 channels; PrP[106–126] (VVAA/SSSS) 88 channels; and PrP[106–126] (Scrambled) 0 channels. These channels were recorded at different voltages ranging between −140 and +160 mV and in solutions of different composition and concentrations. The life span of the channel varied between less than 1 minute and 1 hour. The activity of these channels was lost, mainly because of bilayer breakage, after (a) application of large voltages, particularly positive voltages; (b) ultrasonic mixing of the *cis* and/or *trans* solutions after the addition of a treatment; and (c) perfusion of the *cis* or *trans* chamber with new solutions. Also, to a lesser extent, loss of activity was due to the bilayer thickening that resulted from the increase in the volume of the solvent separating the monolayers of the painted artificial bilayer. The channels formed by PrP[106–126] (AA/SS) and PrP[106–126] (VVAA/SSSS) were stable and irreversibly associated with those lipid bilayers that maintained their specific capacitance of >0.42 pF/cm^2. We found that PrP[106–126] (AA/SS) forms heterogeneous ion channels similar to channels formed by PrP[106–126] (Kourie & Culverson, 2000, Kourie et al., 2001a). The channel-forming properties of the peptides are confirmed by a transient increase in the specific capacitance of the bilayer and the appearance of channel activities. On the other hand, the scrambled PrP[106–126] failed to form channels ($n = 16$) when peptide was directly applied, indicating that channel formation is amino-acid-sequence-dependent. We further ascertained that this was not due to a low probability of peptide incorporation into the lipid bilayer. Liposomes were used to detect the incorporation of the scrambled PrP[106–126] into the bilayer by monitoring the specific capacitance of the lipid bilayer. Although the liposomes were incorporated, as indicated by the transient increase in the specific capacitance, no channel activities were observed for scrambled PrP[106–126] ($n = 14$).

Based on the biophysical characteristics, namely, the resultant ion currents, the channels formed by the PrP[106–126] AA/SS mutant were classified, as shown in Fig. 1, to: (a) outward current with fast kinetics, (b) inwardly-directed current with fast kinetics, (c) outwardly-directed irregular "spiky" current, and (d) time-dependent inactivating current. The activation and inactivation of this current (Fig. 1*D*) becomes more apparent after application of positive and negative pre-pulses (*data not shown*). Table 2 shows the distribution of the observed PrP[106–126] WT, PrP[106–126] (AA/SS) and PrP[106–126] (VVAA/SSSS) channels, each obtained from 10 lots of 20 attempts to record ion channels from optimal bilayers in 250/50 mM KCl *cis/trans* solutions. Table 2 shows the distribution of the total 321 observed PrP[106–126] WT ($n = 137 = 42.6\%$), PrP[106–126] (AA/SS) ($n = 96 = 29.9\%$) and PrP[106–126] (VVAA/SSSS) ($n = 88 = 27.4\%$) channels obtained from 10 lots of 20 attempts to incorporate (by either direct peptide addition or by addition of liposomes as peptide carrier) each one of these peptides into optimal bilayers. Reducing the hydrophobicity of PrP[106–126] WT to PrP[106–126] (AA/SS) resulted in a decline in the number of observed outward currents with the fast kinetics (41%), inwardly-directed currents with fast kinetics (89%) and the time-dependent inactivating current (92%). Reducing the hydrophobicity of PrP[106–126] WT to PrP[106–126] (AAVV/SSSS) resulted in a decline in the number of observed outward currents with the fast kinetics (79%), inwardly-directed currents with fast kinetics (11%) and the time-dependent inactivating current (67%). The number of observed outwardly-directed irregular "spiky" currents increased by approximately 25% for PrP[106–126] (AA/SS) and 27% for PrP[106–126] (AAVV/SSSS).

The outwardly-directed fast kinetic currents with their modes (burst mode, spike mode and mainly-open mode) (*see* Fig. 2*A*), have the opening and closing characteristics of typical ion channels, whereas the irregular spike currents lack such clear opening and closing kinetics. The kinetic modes of the fast kinetic-type channel formed by either

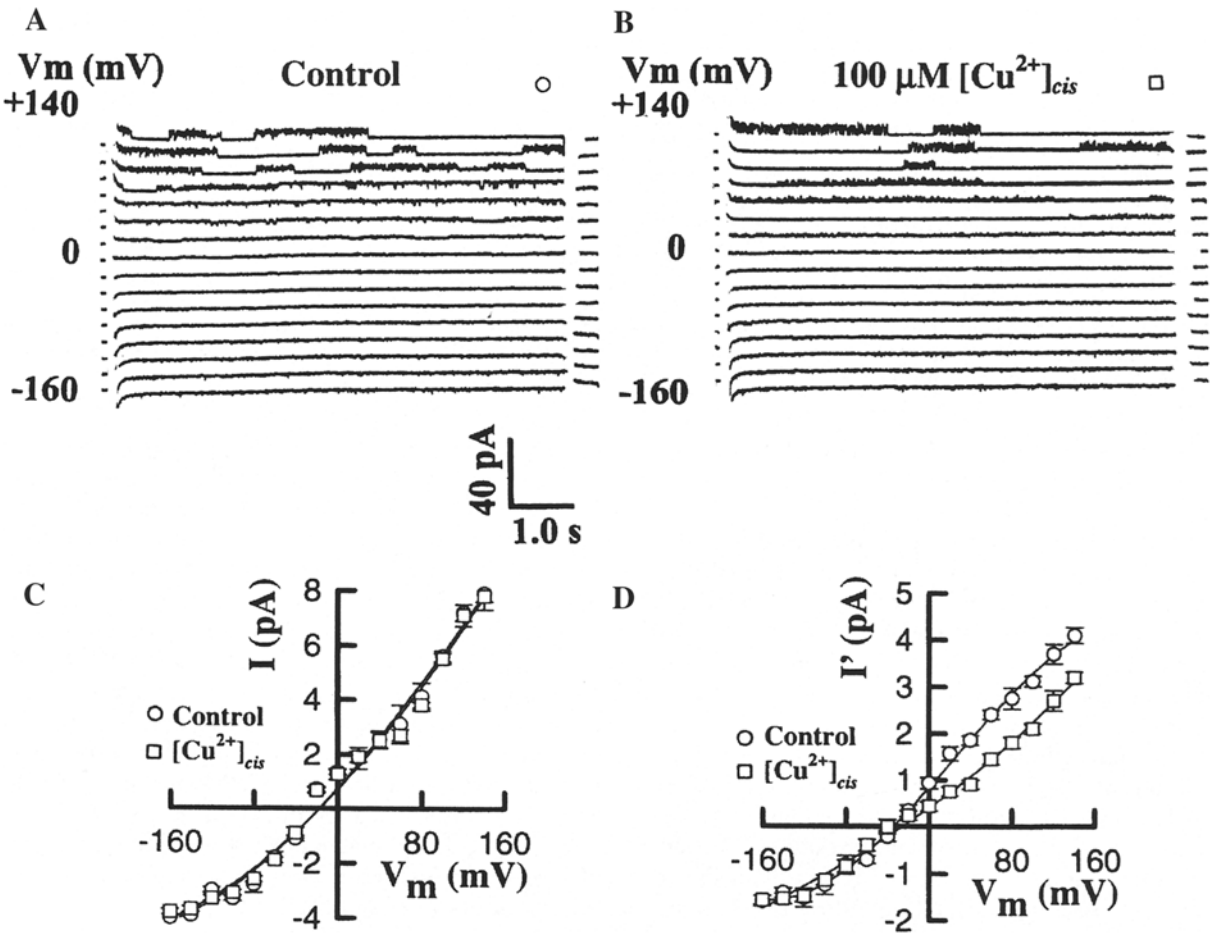

Fig. 2. Effects of $[Cu^{2+}]_{cis}$ on fast cation channels formed by synthetic PrP[106–126] (AA/SS), recorded from voltage-clamped optimal bilayers. (*A*) Control, and (*B*) 100 μM $[Cu^{2+}]_{cis}$. The spike, open and burst kinetic modes of the fast channel are apparent, e.g., at +80 and 100 mV in (*A*). Current-voltage relationships constructed for *I* in (*C*) and *I'* in (*D*). The symbols indicate (○) for control and (□) for 100 μM $[Cu^{2+}]_{cis}$. The vertical bars represent SEM for data obtained from 4–6 channels.

PrP[106–126] (AA/SS) or PrP[106–126] (VVAA/SSS) were similar to those formed with wild-type PrP[106–126], which had been characterized previously (Kourie et al., 2001). The fast kinetic-type channel has a conductance of ~58 pS in 250 mM/50 mM *cis/trans*. The current-voltage relationships for these three modes were nonlinear and fitted by a third-order polynomial. The reversal potential, E_{rev}, ranges between −40 and −10 mV, depending on the goodness of the fit. The only ion present in the *cis* and *trans* solutions that has an equilibrium potential close to these reversal potentials was potassium, thus confirming that the current was carried by K^+. The mutant PrP[106–126] VVAA/SSSS produced 12% of fast-type currents, whereas the more hydrophobic mutant PrP[106–126] (AA/SS) produced 34% fast-type currents. These findings suggest that although a reduction in the hydrophobicity of PrP[106–126] reduces the ability of this peptide to form a fast-type channel, it did not eliminate its ability to interact with and form other ion channel types (Table 2). In contrast, as stated earlier, scrambled PrP[106–126] failed to form ion channels (n = 30; n = 16 with direct peptide addition and n = 14 via liposomes).

Effects of Cu^{2+} on the Conductance of the Fast Channel

To determine whether the hydrophobic core of PrP[106–126] forms a binding site for Cu^{2+}, the effects of Cu^{2+} on ion channels formed by PrP[106–126] mutants were examined. We found that Cu^{2+} modified the kinetics of the fast channel, without affecting current amplitude. These findings are similar to those reported for the deamidated-type of channels formed by PrP[106–126] (Kourie et al., 2001a). In that study, when the channel was in the open mode, Cu^{2+} induced some intrabursts, or long-duration channel closures, in the channel activity at positive voltages. In this study, we observed that Cu^{2+} shifts the kinetics of the fast channel from the burst mode

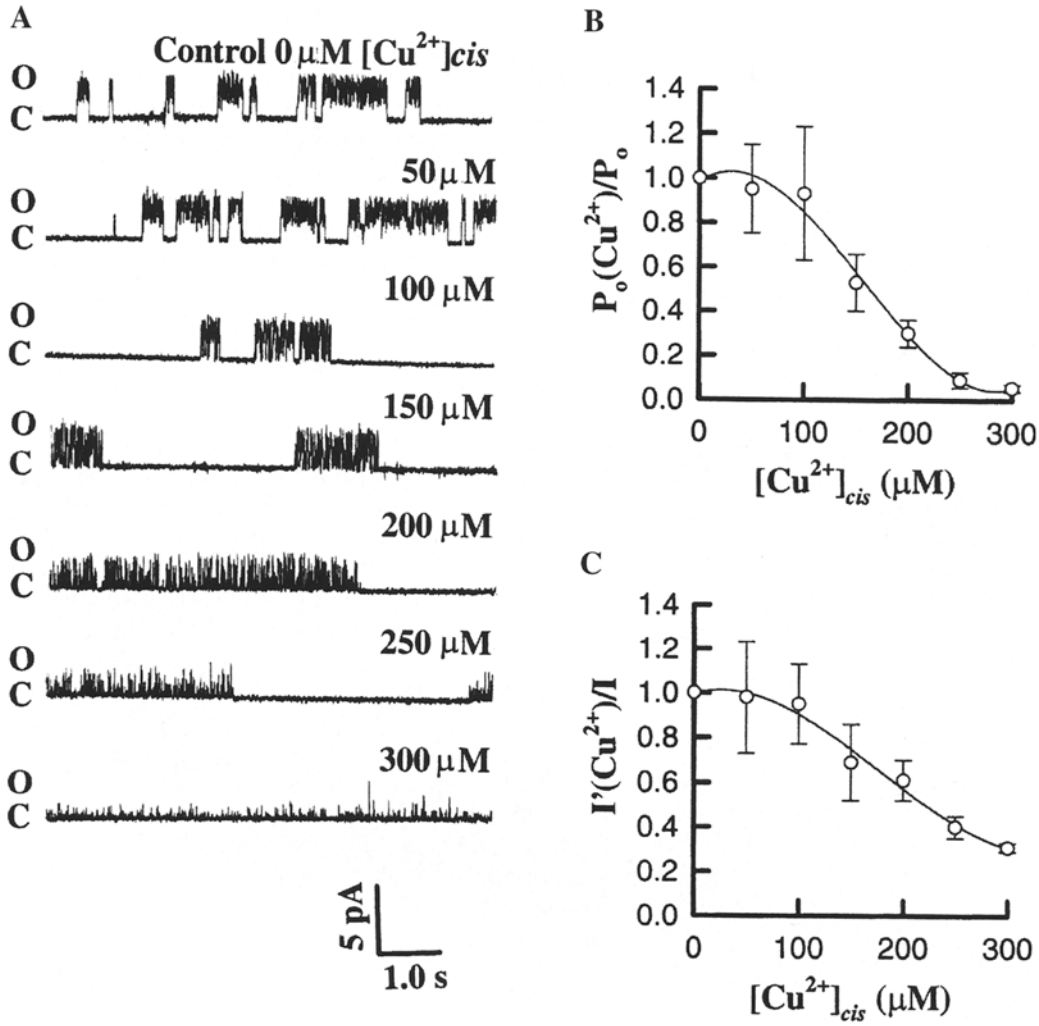

Fig. 3. The inhibitory effects of *cis* Cu^{2+} on the activity of fast channels formed by PrP[106–126] (AA/SS) in the burst mode, activated at V_m of +140 mV in KCl (250 mM/50 mM; *cis/trans*. (*A*) Current traces for control and different $[Cu^{2+}]_{cis}$ between 50 and 300 μM. Following convention, the upward deflections denote activation of outward ion current. *O* and *C* (shown on the left) denote open and closed states of the channel, respectively. For clarity, only one, out of 16, typical current trace is shown at each treatment. For a better display, the data are filtered at 1 kHz, digitized at 2 kHz and reduced by a factor of five. The current traces are separated by a 10 pA offset. Dose-dependent effects of $[Cu^{2+}]_{cis}$ on the PrP[106–126] (AA/SS) fast channel parameter $P_o(Cu^{2+})/P_o$ (*B*) and $I'(Cu^{2+})/I'$ (*C*). The solid lines were fitted by a third-order polynomial. The vertical bars represent SEM for data obtained from 3–5 channels.

(Fig. 2*A*) to a mode having faster transitions between the open and closed states, i.e., spike mode (Fig. 2*B*). The current-voltage relationship constructed for the currents measured in control and in the presence of Cu^{2+} reveal that the current amplitude, maximal conductance ($g_{max} \sim 58$ pS) and the reversal potential (E_{rev}) were not affected by the presence of 50–300 μM $[Cu^{2+}]_{cis}$ (Fig. 2*C*). However, the current-voltage relationship of the average mean current, I' (a parameter that is also dependent on the kinetics of the channel), shows a decrease in the amount of current through this channel at voltages between −20 and +140 mV (Fig. 2*D*). The effects of $[Cu^{2+}]_{cis}$ on the channel activity were reversible (*data not shown*).

$[Cu^{2+}]$-Dependency of the Inhibition of the Fast Channel Type

The inhibitory dose-response of the fast outward current on $[Cu^{2+}]_{cis}$ was examined at several concentrations between 0 and 300 μM on PrP[106–126] AA/SS. The $[Cu^{2+}]_{cis}$ was successively increased by 50 μM increments and families of current traces were obtained at voltages between −160 and +140 mV. Figure 3 shows current traces obtained at +140 mV and in the presence of various $[Cu^{2+}]_{cis}$ between 0 and 300 μM. The time course of these current traces indicates that Cu^{2+} induced rapid transitions between the open and closed states of the channel in a concentration-dependent manner. The induced spike kinetic mode, also known

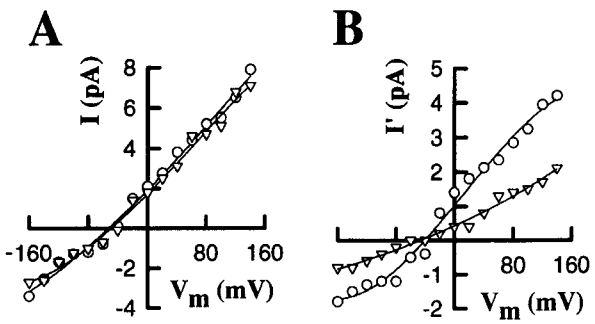

Fig. 4. The effects of different concentrations of *cis* Cu^{2+} on the activity of a PrP[106–126] (AA/SS) fast channel, in the burst mode, activated at different voltages between −160 and +140 mV in KCl (250 mM/50 mM; *cis*/*trans*). Current-voltage relationships for *I* (*A*) and *I'* (*B*). The solid lines are fitted with a third-order polynomial for control (○) and for 300 μM Cu^{2+} (▽). For clarity, the *I-V* curves for the $[Cu^{2+}]_{cis}$ of 50, 100, 150, 200 and 250 μM, which lie between control (○) and 300 μM (▽), are not shown. These *I-V* curves showed no significant changes in the reversal potentials, E_{rev}.

as a "flicker mode", is characteristic of a fast block mechanism that occurs when an agent binds to the mouth of the channel, affecting its kinetics but not its conductance. These findings indicate that the open state of the PrP[106–126]-mutant channel was voltage-dependent and that Cu^{2+} could have acted on the open state of the channel. The estimated K_{d50} values obtained from the dose-dependent plots of the ratios $P_o(Cu^{2+})/P_o$ and $I'(Cu^{2+})/I'$ were 164.4 ± 8.7 and 213 ± 13.9 μM, respectively (Fig. 3*B* and *C*). These findings confirm that the kinetic properties of this channel type are more sensitive to increases in $[Cu^{2+}]_{cis}$ than are its conductance properties.

Current-Voltage Relations of the Fast Channel Type at Different *cis* Cu^{2+}

The current-voltage relationships constructed from ion current families, obtained at different voltages, show weak outward rectification of *I* and *I'* and confirm the increase in current amplitude at depolarizing voltages (Fig. 4*A* and *B*). It is apparent that the *I* and the weak rectification have not been affected by 0–300 μM $[Cu^{2+}]_{cis}$ (Fig. 4*A*). On the other hand, the physiologically important *I'* has been reduced at both positive and negative voltages. The current reversal potential (E_{rev}) in the presence of 0–300 μM $[Cu^{2+}]_{cis}$ remained steady and close to E_K, the reversal potential for K^+ (Fig. 4*A* and *B*). The reversal potentials for *I* of the PrP[106–126] (AA/SS) fast cation channel in control and different $[Cu^{2+}]_{cis}$ were between −37.4 and −39.5 mV.

Effects of Cu^{2+} on the Kinetics of the Fast Channel Type

The kinetic parameters describing the channel activity were obtained at voltages between −160 and +140 mV and in the absence and presence of different Cu^{2+} concentrations (Fig. 5). Cu^{2+} modified the kinetic parameters of the fast channel in the burst mode. At positive voltages between 0 and +140 mV, Cu^{2+} decreased the values of P_o and T_o (Fig. 5*A* and *C*) and increased the values of F_o and T_c (Fig. 5*B* and *D*). The Cu^{2+}-induced voltage-dependent changes in P_o (Fig. 5*A*) were primarily due to decreases in the values of T_o and increases in T_c (Fig. 5*C* and *D*).

The Secondary Structure of PrP[106–126] (AA/SS) and PrP[106–126] (VVAA/SSSS) in Lipid Membranes

Figure 6*A* shows the CD spectra of freshly prepared PrP[106–126] in negatively charged LUV. The spectrum has a minimum at 225 nm that is consistent with a predominately β-sheet secondary structure. The CD spectra (Fig. 6*A*) of the mutant peptides AA/SS and VVAA/SSSS indicate that the secondary structure of these peptides in lipid environments is significantly different from that of the native sequence; these peptides have a mixture of random coil, α-helical and β-sheet structures.

When Cu^{2+} was added, only minimal change was observed in the CD spectrum of PrP[106–126] in LUV. On the addition of Cu^{2+} to AA/SS VVAA/SSSS in LUV the CD spectra showed a significant reduction in the β-sheet component of the secondary structure.

Discussion

The main finding of this study was that a reduction in the hydrophobicity of the PrP[106–126] sequence modifies the distribution of the ion channels formed, resulting in a decrease in the outwardly-directed and the time-dependent inactivating current and an increase in the outwardly-directed irregular 'spiky' currents. The PrP[106–126]-mutant ion channels maintain their sensitivity to Cu^{2+} (Figs. 1–3), as has been reported previously, (Kourie et al., 2001a). The changes in the distribution of formed channels having different conductance and kinetic properties could explain the decrease in neurotoxicity that was correlated with changes in secondary structure, fibril formation, and amyloidogenicity of the mutant peptides (Jobling et al., 1999). In this study, we found a significant decrease in the formation of fast-kinetic channels for the PrP[106–126] (AAVV/SSSS) mutant. The mechanism of changes in the secondary structure-related decrease in channel formation could be mediated by a decline in the hydrophobicity essential for peptide-lipid interaction and β-sheet-based channel formation. This is consistent with the CD studies in LUV (Fig. 6), which confirmed that the mutant peptide had significantly less β-sheet structure than

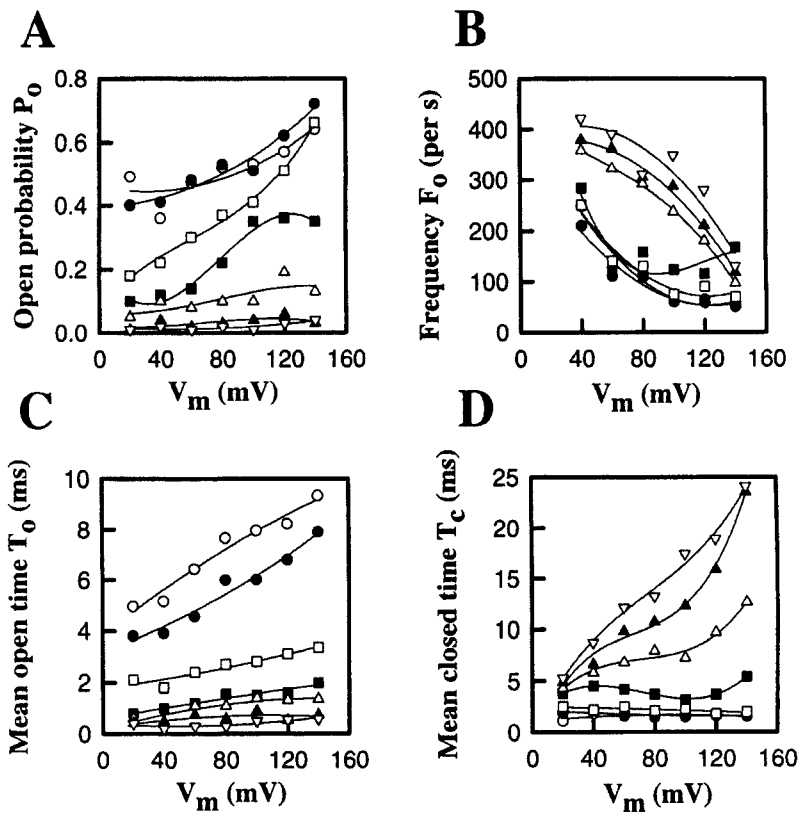

Fig. 5. Effects of different $[Cu^{2+}]_{cis}$ on the voltage-dependence of the kinetic parameters of PrP[106–126] (AA/SS) fast channels in the burst mode, activated at different voltages in KCl (250 mM/50 mM; *cis/trans*). (*A*) Open probability (P_o), (*B*) frequency of opening (F_o), (*C*) mean open time (T_o), and (*D*) mean closed time (T_c). The solid lines are fitted with a second-order polynomial for control (○) and for the different $[Cu^{2+}]_{cis}$ at 50 (●), 100 (□), 150 (■), 200 (△), 250 (▲), and 300 μM (▽). The threshold for channel detection was set at 50% of the current amplitude.

the native sequence. The significance of the hydrophobic region in structure-toxicity relationships has been reported for both PrP (Jobling et al., 1999) and Aβ (Pike et al., 1995). We suggest that the hydrophobic cores of PrP[106–126] and the Aβ25–35 have an important role in the incorporation and stabilization of aggregated peptide channels that are capable of inducing neurotoxicity.

The data presented in this study suggest a role for the hydrophobic core in channel-type formation and it eliminates this region as a possible modulator of the sensitivity to Cu^{2+} of fast-kinetic channel formed by PrP[106–126]. The diversity of the channels formed (Fig. 1) and the biophysical properties are similar to those of channels formed by other amyloid proteins (Kourie et al., 2001b). These similarities could be relevant to a general mechanism of action of these amyloids. It has been proposed that the inherent toxicity of aggregates and intermediates constitute a common mechanism for protein-misfolding diseases (Bucciantini et al., 2002). We propose that these structural configurations confer upon these aggregates and their intermediates the ability to form heterogeneous ion channels (Fig. 1), which underlies a common mechanism for misfolding diseases. The common structural changes of misfolded proteins include the exposure of hydrophobic regions and charged residues needed for the formation of β sheet-based intermediates that are capable of interacting with cellular membranes. Several aggregation-prone peptide intermediates form ion channels with similar biophysical properties that could indicate shared channel structures (Kourie et al., 2001a, b). We therefore propose that the mechanism of aggregation-triggered channel formation mediates membrane damage and represents a general mechanism to explain other malfunctioning protein-related pathologies (Kourie & Henry, 2001, 2002). Recently, evidence obtained using electron microscopy and CD techniques confirm that different amyloid-forming peptides share structural features such as β sheet-based pore-like protofibrils that have been suggested to be related to their toxicity (Lashuel et al., 2002). In accordance with the pore-forming toxins that have β sheet-based structures, Hirakura et al., (2000) proposed that PrP[106–126] forms β sheets that aggregate prior to the formation of a channel whose structure is thought to be that of a β barrel. A model for such β-barrel pathogenic prion channels has been proposed (Chapron et al., 2000). Similarly, the relationship between ion channels and the physicochemical properties of amyloid peptides has also been studied in the 40- to 42-amino acid amyloid β peptide (Aβ) of Alzheimer's disease (*see* Durrell et al., 1994). The findings of several Aβ studies are in agreement with the proposed role of the hydrophobic region of PrP[106–126] reported in this study. The hydrophobic region 29–35 of the channel-forming fragment Aβ25–35 modulated the secondary structure and the stable aggregation of the peptide, which in turn altered its neurotoxicity (Pike et al., 1995). Mutagenesis of the hydrophobic core of Aβ also reduced the peptide's

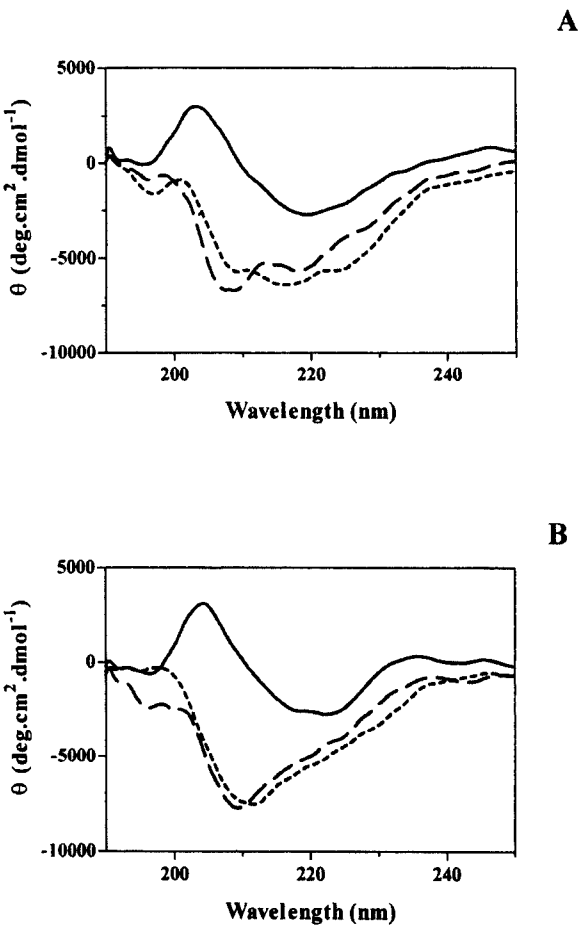

Fig. 6. CD spectra of PrP[106–126] in LUVs (*A*) in the absence and (*B*) in the presence of Cu^{2+}. The solid line represents the wild-type PrP[106–126], the dotted line represents the mutant PrP[106–126] (AA/SS) and the dashed line represents the mutant PrP[106–126] (VVAA/SSSS).

β-sheet content and its fibrillogenic properties (Hilbich et al., 1992) and ion channel function (Durrell et al., 1994). This may occur by intermolecular interactions involved in forming the β-pleated sheet that are dependent upon hydrophobic interactions (Barrow & Zagorski, 1991; Barrow et al., 1992) and could be influencing membrane incorporation and ion channel formation.

The Cu^{2+}-induced changes in the kinetics of the channels formed by the PrP[106–126] AA/SS mutant (Fig. 2) is consistent with Cu^{2+} binding to a hydrophilic site at the cytoplasmic mouth of the PrP[106–126] channel (Kourie et al., 2001). M_{109} and H_{111} are part of a binding site for Cu^{2+} (Jobling et al., 1999, 2001) and their close proximity to the N-terminus is consistent with this site being located at the mouth of the channel. The presence of the Cu^{2+}-binding site near the N-terminus of PrP[106–126] is also in agreement with previous findings showing the binding of divalent ions to other channel-forming amyloids, e.g., CNP-39(1–17) (*see* Kourie, 1999). If Cu^{2+}-modulated prion channels could be formed and function in vivo in a manner similar to that of PrP[106–126] (Fig. 2), then they could modify the resting membrane potential and the action potential. The PrP[106–126] channels could affect the action potential and the subsequent refractory period so that the neuronal cells would remain in the depolarized state, in a low excitable state, which could explain the PrP[106–126]-induced increase in $[Cu^{2+}]_i$ (*see* Florio et al., 1996). In neurons, PrP[106–126] channels might cause frequency-dependent failure of voltage-dependent neurosecretion (*see* Barrow et al., 1999). The heterorganic nature, indicated by the differences in conductance, selectivity and kinetics, of the PrP[106–126] channels insures the cytotoxic effects of this peptide.

I thank Dr. W.L.F. Armarego, and Mr. R. McCart and Mr. H. for suggestions and critical reading of the manuscript. The laboratory assistance of Ms. R. Bahadi, Ms. K.N. Laohachai and Mr. P.V. Farrelly is greatly appreciated. This research work is supported by National Health and Medical Research Council project grants (970122 and 120808) and Australian Research Council Small Research Grant (F99123 and F0047).

References

Arispe, N., Pollard, H.B., Rojas, E. 1996. Zn^{2+} interaction with Alzheimer amyloid beta protein calcium channels. *Proc. Natl. Acad. Sci. USA* **93:**1710–1715

Barrow, C.J., Yasuda, A., Kenny, P.T., Zagorski, M.G. 1992. Solution conformations and aggregational properties of synthetic amyloid beta-peptides of Alzheimer's disease. Analysis of circular dichroism spectra. *J. Mol. Biol.* **225:**1075–1093

Barrow, C.J., Zagorski, M.G. 1991. Solution structures of beta peptide and its constituent fragments: relation to amyloid deposition. *Science* **253:**79–182

Barrow, P.A., Holmgren, C.D., Tapper, A.J., Jefferys, J.G. 1999. Intrinsic physiological and morphological properties of principal cells of the hippocampus and neocortex in hamsters infected with scrapie. *Neurobiol. Dis.* **6:**406–423

Barry, P.H. 1994. JPCalc, a Software package for calculating liquid junction potential corrections in patch-clamp, intracellular, epithelial and bilayer measurements and for correcting junction potential measurements. *J. Neurosci. Meth.* **51:**107–116

Brown, D.R., Clive, C., Haswell, S.J. 2001. Antioxidant activity related to copper binding of native prion protein. *J. Neurochem.* **76:**69–76

Brown, D.R., Herms, J., Kretzschmar, H.A. 1994. Mouse cortical cells lacking cellular PrP survive in culture with a neurotoxic PrP fragment. *Neuroreport* **5:**2057–2060

Bucciantini, M., Giannoni, E., Chiti, F., Baroni, F., Formigli, L., Zurdo, J., Taddei, N., Ramponi, G., Dobson, C.M., Stefani, M. 2002. Inherent toxicity of aggregates implies a common mechanism for protein misfolding diseases. *Nature* **416:**507–511

Bush, A.I. 2000. Metals and neuroscience. *Curr. Opin. Chem. Biol.* **4:**184–191

Chapron, Y., Peyrin, J.M., Crouzy, S., Jaegly, A., Dormont, D. 2000. Theoretical analysis of the implication of PrP in neuronal death during transmissible subacute spongiform encephalopathies: hypothesis of a PrP oligomeric channel. *J. Theor. Biol.* **204:**103–111

Colquhoun, D., Hawkes, A.G. 1983. Fitting and statistical analysis of single-channel recording. *In:* Single Channel Recording. B.

Sakmann and E. Neher, editors. pp. 135–175. Plenum, New York

Durell, S.R., Guy, H.R., Arispe, N., Rojas, E., Pollard, H.B. 1994. Theoretical models of the ion channel structure of amyloid beta-protein. *Biophys. J.* **67:**2137–2145

Florio, T., Grimaldi, M., Scorziello, A., Salmona, M., Bugiani, O., Tagliavini, F., Forloni, G., Schettini, G. 1996. Intracellular calcium rise through L-type calcium channels, as molecular mechanism for the prion protein fragment 106–126-induced astroglial proliferation. *Biochem. Biophys. Res. Commun.* **228:**397–405

Forloni, G., Del Bo, R., Angeretti, N., Smiroldo, S., Gabellini, N., Vantini, G. 1993. Nerve growth factor does not influence the expression of beta amyloid precursor protein mRNA in rat brain: in vivo and in vitro studies. *Brain. Res.* **620:**292–296

Gu, Y., Fujioka, H., Mishra, R.S., Li, R., Singh, N. 2002. Prion peptide 106–126 modulates the aggregation of cellular prion protein and induces the synthesis of potentially neurotoxic transmembrane PrP. *J. Biol. Chem.* **277:**2275–2286

Hilbich, C., Kisters-Woike, B., Reed, J., Masters, C.L., Beyreuther, K. 1992. Substitutions of hydrophobic amino acids reduce the amyloidogenicity of Alzheimer's disease beta A4 peptides. *J. Mol. Biol.* **228:**460–473

Hirakura, Y., Yiu, W.W., Yamamoto, A., Kagan, B.L. 2000. Amyloid peptide channels: blockade by zinc and inhibition by Congo red (amyloid channel block). *Amyloids* **3:**194–199

Jobling, M.F., Huang, X., Stewart, L.R., Barnham, K.J., Curtain, C.C., Volitakis, I., Perugini, M., White, A.R., Cherny, R.A., Masters, C.L., Barrow, C.J., Collins, S.J., Bush, A.I., Cappai, R. 2001. Copper and zinc binding modulates the aggregation and neurotoxic properties of the prion peptide PrP106–126. *Biochem.* **40:**8073–8084

Jobling, M.F., Stewart, L.R., White, A.R., McLean, C., Friedhuber, A., Maher, F., Beyreuther, K., Masters, C.L., Barrow, C.J., Collins, S.J., Cappai, R. 1999. The hydrophobic core sequence modulates the neurotoxic and secondary structure properties of the prion peptide 106–126. *J. Neurochem.* **73:**1557–1565

Kawahara, M., Kuroda, Y., Arispe, N., Rojas, E. 2000. Alzheimer's disease-amyloid, human islet amylin, and prion protein fragment evoke intracellular free calcium elevations by a common mechanism in hypothalamic GnRH neuronal cell line. *J. Biol. Chem.* **275:**14077–14083

Kourie, J.I. 1996. Vagaries of artificial bilayers and gating modes of the SCl channel from the sarcoplasmic reticulum muscle. *J. Membr. Sci.* **116:**221–227

Kourie, J.I. 1999. Calcium dependence of C-type natriuretic peptide-formed fast K^+ channel. *Am. J. Physiol.* **277:**C43–C50

Kourie, J.I. 2001. Mechanisms of prion-induced modification in membrane transport systems. *Chemico-Biological Interactions* **138:**1–26

Kourie, J.I., Culverson, A. 2000. Prion peptide fragment PrP[106–126] forms distinct cation channel types. *J. Neurosci. Res.* **62:**120–133

Kourie, J.I., Farrelly, P.V., Henry, C.L. 2001a. Channel activity of deamidated isoforms of prion protein fragment 106-126 in planar lipid bilayers. *J. Neurosci. Res.* **66:**214–220

Kourie, J.I., Henry, C.L. 2001. Protein aggregation and deposition: Implications for ion channel formation and membrane damage. *Crot. Med. Res.* **42:**358–373

Kourie, J.L., Henry, C.L. 2002. Ion channel formation and membrane-linked pathologies of misfolded hydrophobic proteins: The role of dangerous unchaperoned molecules. *Clin. Exp. Pharmacol. Physiol.* **29:**741–753

Kourie, J.I., Henry, C.L., Farrelly, P.V. 2001b. Diversity of amyloid β protein fragment [1-40]-formed channels. *Cell. Mol. Neurobiol.* **21:**255–284

Kourie, J.I., Laver, D.R., Junankar, P.R., Gage, P.W., Dulhunty, A.F. 1996. Characteristic of two types of chloride channel in sarcoplasmic reticulum vesicles from rabbit skeletal muscle. *Biophys. J.* **70:**202–221

Lashuel, H.A., Hartley, D., Petre, B.M., Walz, T., Lansbury P.T. Jr. 2002. Neurodegenerative disease: amyloid pores from pathogenic mutations. *Nature* **418:**291

Lin, M.-C., Mirzabekov, T., Kagan, B.L. 1997. Channel formation by a neurotoxic prion protein fragment. *J. Biol. Chem.* **272:**44–47

Miller, C., Racker, E. 1976. Ca^{++}-induced fusion of fragmented sarcoplasmic reticulum with artificial planar bilayers. *J. Membrane Biol.* **30:**283–300

Mobashery, N., Nielsen, C., Andersen, O.S. 1997. The conformational preference of gramicidin channels is a function of lipid bilayer thickness. *FEBS Lett.* **412:**15–20

Pan, K.-M., Baldwin, M., Nguyen, J., Gasset, M., Serban A., Groth D., Melhorn I., Huang Z., Flettenck R.J., Cohen F.E., Prusiner S.B. 1993. Conversion of α-helices into β-sheets features in the formation of the scrapie prion proteins. *Proc. Natl. Acad. Sci. USA* **90:**10962–10966

Patlak, J.B. 1993. Measuring kinetics of complex single ion channel data using mean-variance histograms. *Biophys. J.* **65:**29–42

Pike, C.J., Walencewicz-Wasserman, A.J., Kosmoski, J., Cribbs, D.H., Glabe, C.G., Cotman, C.W. 1995. Structure-activity analyses of β-amyloid peptides: contributions of the β25–35 region to aggregation and neurotoxicity. *J. Neurochem.* **64:**253–265

Prusiner, S.B., Scott, M.R., DeArmond, S.J., Cohen, F.E. 1998. Prion protein biology. *Cell* **93:**337–348

Singh, N., Gu, Y., Bose, S., Kalepu, S., Mishra, R.S., Verghese, S. 2002. Prion peptide 106–126 as a model for prion replication and neurotoxicity. *Front. Biosci.* **7:**60–71

Stewart, L.R., White, A.R., Jobling, M.F., Needham, B.E., Maher, F., Thyer, J., Beyreuther, K., Masters, C.L., Collins, S.J., Cappai, R. 2001. Involvement of the 5-lipoxygenase pathway in the neurotoxicity of the prion peptide PrP106-126. *J. Neurosci.* **65:**565–572

Tagliavini, F., Forloni, G., Bugiani, O., Salmona, M. 2001. Studies on peptide fragments of prion proteins. *Adv. Protein Chem.* **57:**171–201

Warwicker, J. 1999. Modelling charge interactions in prion protein: predictions for pathogenesis. *FEBS Lett.* **450:**144–148

White, A.R., Guirguis, R., Brazier, M.W., Jobling, M.F., Hill, A.F., Beyreuther, K., Barrow, C.J., Masters, C.L., Collins, S.J., Cappai, R. 2001. Sublethal concentrations of prion peptide PrP106–126 or the amyloid beta peptide of Alzheimer's disease activates expression of proapoptotic markers in primary cortical neurons. *Neurobiol. Dis.* **8:**299–316

Wong, B.-S., Pan, T., Liu, T., Li, R., Petersen, R.B., Jones, I.M., Gambetti, P., Brown, D.R., Sy, M.-S. 2000. Prion disease: A loss of antioxidant function. *Biochem. Biophys. Res. Commun.* **275:**249–252